

## Electronic Entanglement in Late Transition Metal Oxides

Patrik Thunström, Igor Di Marco, and Olle Eriksson

*Department of Physics and Astronomy, Uppsala University, Box 516, SE-75120 Uppsala, Sweden*

(Received 27 February 2012; published 31 October 2012)

We present a study of the entanglement in the electronic structure of the late transition metal monoxides—MnO, FeO, CoO, and NiO—obtained by means of density-functional theory in the local density approximation combined with dynamical mean-field theory. The impurity problem is solved through exact diagonalization, which grants full access to the thermally mixed many-body ground state density operator. The quality of the electronic structure is affirmed through a direct comparison between the calculated electronic excitation spectrum and photoemission experiments. Our treatment allows for a quantitative investigation of the entanglement in the electronic structure. Two main sources of entanglement are explicitly resolved through the use of a fidelity based geometrical entanglement measure, and additional information is gained from a complementary entropic entanglement measure. We show that the interplay of crystal field effects and Coulomb interaction causes the entanglement in CoO to take a particularly intricate form.

DOI: [10.1103/PhysRevLett.109.186401](https://doi.org/10.1103/PhysRevLett.109.186401)

PACS numbers: 71.20.Be, 03.67.Mn, 71.15.-m, 71.27.+a

Entanglement is a fundamental aspect of quantum mechanics, responsible for a large range of complex phenomena not present in a classical setting. The entanglement of distinguishable particles was historically seen as something spooky, but is now considered a valuable resource. It plays an essential role in quantum information theory, and has been studied in great detail both theoretically and experimentally [1]. Entanglement of indistinguishable particles has received less explicit attention, but it has been studied indirectly in both the quantum chemistry and condensed matter communities. Describing the electronic structure of materials with a pure separable state, represented as a single Slater determinant, is at the very heart of the modern computational approaches, and the inability to do so is known under the term *correlation*. The term encompasses both classical and quantum correlations (entanglement), where the former results in mixed states and the latter in entangled states. The presence of entanglement is usually considered a computational complication as it prevents the use of these standard approaches. The development of reliable computational methods and entanglement measures are of key importance to turn also the entanglement of indistinguishable particles from a complication into a potential resource.

Well known examples of strongly correlated materials are the late transition metal monoxides (TMOs)—MnO, FeO, CoO, and NiO—which have been under intense experimental and theoretical attention for a long time [2–4]. Here we report on a theoretical description of the late TMOs using the local density approximation (LDA) plus dynamical mean field theory (DMFT) [5] where the effective impurity model is solved by exact diagonalization (ED) [6]. The quality of the results is assessed through a direct comparison between the computed spectral function

and photoemission experiments [x-ray photoemission spectroscopy (XPS) or bremsstrahlung isochromat spectroscopy (BIS)]. We then take advantage of the direct access to the local many-body ground state of the impurity problem to analyse the entanglement in detail.

The LDA + DMFT scheme is built around the mapping of the local lattice problem to an effective impurity problem. The impurity system is described in ED through the local projected LDA Hamiltonian  $\hat{H}_{ij}^{\text{LDA}}$ , a double counting term  $\hat{H}_{ij}^{\text{DC}}$ , the on-site Coulomb interaction  $\hat{U}$ , and a few auxiliary bath states, giving the Hamiltonian

$$\hat{H}^{\text{ED}} = \sum_{ij} (\tilde{H}_{ij}^{\text{LDA}} - \tilde{H}_{ij}^{\text{DC}}) \hat{c}_i^\dagger \hat{c}_j + \frac{1}{2} \sum_{ijkl} \tilde{U}_{ijkl} \hat{c}_i^\dagger \hat{c}_j^\dagger \hat{c}_i \hat{c}_k + \sum_{im} (\tilde{V}_{im} \hat{c}_i^\dagger \hat{c}_m + \text{H.c.}) + \sum_m \tilde{E}_m \hat{c}_m^\dagger \hat{c}_m, \quad (1)$$

where the indices  $i, j, k, l$  run over the local correlated orbitals and  $m$  runs over the auxiliary bath states. The energies  $E_m$  and the hybridization strength  $V_{im}$  of the auxiliary bath states mimic the hybridization between the TM-3d and the O-2p and O-2s orbitals. The Hamiltonian of the finite system is diagonalized numerically to produce an analytical self-energy. The calculations were carried out in the paramagnetic (PM) phase, using a finite temperature ( $\beta = 0.00173$  Ry) fully charge self-consistent LDA + DMFT implementation [7–10]. Further technical details, including the parametrization of  $\tilde{U}_{ijkl}$  and the fitting of  $E_m$  and  $V_{im}$ , can be found in the Supplemental Material [11].

In Fig. 1 the calculated projected spectral function of the TM-3d and O-2p states are compared to experimental XPS (electron removal) and BIS (electron addition) data [12,13] showing mainly the contribution of the TM-3d states, due to the photon energies used. The overall agreement for MnO, CoO, and NiO is excellent, and even minor

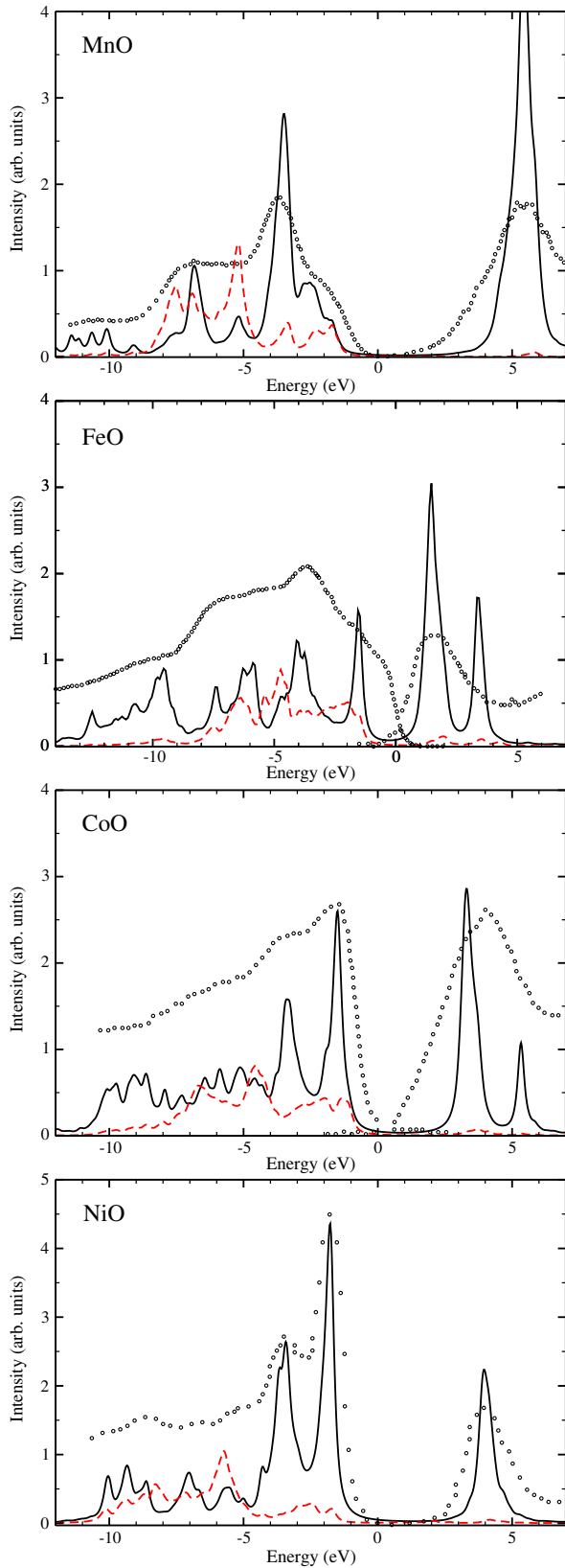


FIG. 1 (color online). Spectral function of the TM 3d states (thick black lines) and O 2p states (dashed red lines) in MnO, FeO, CoO, and NiO, and corresponding XPS/BIS data (black circles) [12,13]. The Fermi level is at zero energy.

experimental features like the high energy satellites are found in our theory. The CoO sample used in the experiment was doped with 1% Li to avoid charging effects. However, this doping gives rise to  $\text{Co}_3\text{O}_4$ -like domains in the sample, which contribute to the early onset seen in the BIS spectrum [13]. The projected spectral function of FeO shows an acceptable agreement with the experimental spectrum, although the relative intensities could be improved. A greater concern is that the initial shoulder at  $-0.5$  eV is missing and that the peak at 3.5 eV is not evident in the experimental data. However, this may be related to the fact that the experiment was performed with a nonstoichiometric sample ( $\text{Fe}_{0.95}\text{O}$ ) containing  $\text{Fe}_3\text{O}_4$ -like domains [14,15], in contrast to the conventional FeO unit cell used in the calculation. Nevertheless, it can not be ruled out that these features are beyond what can be described with the current method.

Given the satisfactory comparison of the spectral properties with experimental data, we now turn our attention to the entanglement in the thermal many-body ground state of the impurity problem, described by the density operator  $\hat{\rho}^T = e^{-\beta H^{\text{ED}}} / \text{Tr}(e^{-\beta H^{\text{ED}}})$ . Before we start, let us, for clarity, briefly recapitulate the definitions of pure, mixed, separable, and entangled [16]  $N$ -electron many-body states. A pure state is a state which can be described by a state vector  $|\Psi\rangle$ , while a mixed state requires the use of a density operator  $\hat{\rho}$ . A mixed state is said to be classically correlated as its components are related through classical probabilities. A separable (nonentangled) pure state  $|\Psi'\rangle$  can be written as a single Slater determinant [1], while an entangled pure state  $|\Psi\rangle$  requires a superposition of several Slater determinants. An entangled state is said to be quantum correlated as the superposition between its components is a quantum mechanical phenomenon. Finally, a separable mixed state can be written in a diagonal form  $\hat{\rho}' = \sum_i p_i |\Psi'_i\rangle\langle\Psi'_i|$  using only separable component states  $|\Psi'_i\rangle$ , while an entangled mixed state requires at least one entangled component [1]. A key point in the definition of mixed state entanglement is that a classical mixture of any two separable states remains separable.

There exist several ways to measure the entanglement in an  $N$ -electron many-body state [1]. In the case of a pure state  $|\Psi\rangle$ , we first look at the geometric entanglement measure [17]

$$E_G[|\Psi\rangle\langle\Psi|] = 1 - \max_{|\Psi'\rangle} |\langle\Psi'|\Psi\rangle|^2, \quad (2)$$

where  $|\Psi'\rangle$  is restricted to be pure and separable. From a computational point of view this measure is natural since  $|\Psi'\rangle$  corresponds to the best possible single Slater determinant description of the system. We perform the search for the optimal  $|\Psi'\rangle$  by recursively removing one electron at a time from the natural orbitals of the many-body state [11]. Although this procedure is, in general, not guaranteed to find the optimal  $|\Psi'\rangle$ , it is exact for separable states and for pure 2-electron systems.

In order to analyse the thermal density operator  $\hat{\rho}^T$ , it is necessary to generalize the entanglement measure  $E_G$  in Eq. (2) to mixed states. This can be achieved by replacing the overlap with the fidelity [18] between  $\hat{\rho}^T$  and any separable state  $\hat{\rho}'$ ,

$$E_G[\hat{\rho}^T] = 1 - \max_{\hat{\rho}'} \text{Tr}[\sqrt{\sqrt{\hat{\rho}^T} \hat{\rho}' \sqrt{\hat{\rho}^T}}]^2, \quad (3)$$

where  $\hat{\rho}' = \sum_i p_i |\Psi'_i\rangle\langle\Psi'_i|$ ,  $\sum_i p_i = 1$ , and  $|\Psi'_i\rangle$  are separable states. Performing the restrained maximization in Eq. (3) is a formidable task, as one has to consider the effect of mixing several nonorthogonal separable states. However, the problem can be simplified in the PM phase of a system with negligible spin-orbit interaction by noting that  $\hat{H}^{\text{ED}}$  then commutes with  $\hat{S}^2$ ,  $\hat{S}_z$  and its ladder operators  $\hat{S}^\pm$ . This implies that there is a common eigenbasis in which the many-body eigenstates  $|\Psi_{i,m_s}^s\rangle$  can be indexed by  $s(s+1) = \langle\hat{S}^2\rangle$ , and  $m_s = \langle\hat{S}_z\rangle$ , and that the eigenvalues  $E_i^s$  are independent of  $m_s$ . If the system has a well-defined spin moment, e.g., due to a strong on-site Hund's coupling, its thermal density matrix is composed of a mixture of several degenerate eigenstates, all with the same spin quantum number  $s$

$$\hat{\rho}^T = \sum_i p_i \hat{\rho}_i^T = \sum_i \frac{p_i}{2s+1} \sum_{m_s=-s}^s |\Psi_{i,m_s}^s\rangle\langle\Psi_{i,m_s}^s|. \quad (4)$$

We also observe that the spin-coherent operator  $\hat{S}_\lambda = \exp(\lambda\hat{S}^-)(1 + |\lambda|^2)^{-\hat{S}_z}$  conserves the entanglement [11] of the maximally spin-polarized state  $|\Psi_{i,s}^s\rangle$ . Setting  $\lambda_m = \exp[2i\pi m/(2s+1)]$  yields

$$\hat{\rho}_i^T = \sum_{m=-s}^s \frac{\hat{\rho}_i^{\lambda_m}}{2s+1} \equiv \sum_{m=-s}^s \frac{\hat{N}_z \hat{S}_{\lambda_m} |\Psi_{i,s}^s\rangle\langle\Psi_{i,s}^s| \hat{S}_{\lambda_m}^\dagger \hat{N}_z^\dagger}{2s+1}, \quad (5)$$

where

$$\hat{N}_z = 2^s / \sqrt{\binom{2s}{s - \hat{S}_z}} (2s+1)$$

When applying the proposed Slater search algorithm to the pure state  $\hat{\rho}_i^{\lambda_m}$  of the TMOs, the maximal overlap is always obtained for  $\hat{S}_{\lambda_m} |\Psi_{i,s}^{s'}\rangle$ , where  $|\Psi_{i,s}^{s'}\rangle$  is the closest separable state to  $|\Psi_{i,s}^s\rangle$ . Hence, the separable state

$$\hat{\rho}'_i = \frac{1}{2s+1} \sum_{m=-s}^s \hat{S}_{\lambda_m} |\Psi_{i,s}^{s'}\rangle\langle\Psi_{i,s}^{s'}| \hat{S}_{\lambda_m}^\dagger, \quad (6)$$

gives a local minimum of  $E_G[\hat{\rho}'_i]$ . Moreover, each term  $\hat{\rho}_i^{\lambda_m}$  contains the same amount of entanglement, originating from the material specific  $|\Psi_{i,s}^s\rangle$  and the action of the renormalization operator  $\hat{N}_z$ . Therefore we conjecture that the local minimum given by  $\hat{\rho}'_i$  is in fact a global minimum. The geometric entanglement measure for the PM state  $\hat{\rho}^T$  can then be written as [11]

$$E_G[\hat{\rho}^T] = 1 - \frac{1 - E_G[\hat{\rho}_s^T]}{2^{2s}(2s+1)} \left[ \sum_{m=-s}^s \sqrt{\binom{2s}{s-m}} \right]^2, \quad (7)$$

where  $\hat{\rho}_s^T = \sum_i p_i |\Psi_{i,s}^s\rangle\langle\Psi_{i,s}^s|$ . Even when  $E_G[\hat{\rho}_s^T]$  is zero there is still a nontrivial term remaining in Eq. (7). This source of entanglement is very robust as it does not depend on the details of the electronic structure of the system but only on  $\langle\hat{S}^2\rangle$ .

As a complement to the geometric entanglement measure we have used an entropic measure, based on the reduction of the many-body density matrix  $\hat{\rho}$  to the one-particle reduced density matrix  $\tilde{\rho}_{ij} = \text{Tr}(\hat{\rho} c_j^\dagger c_i)$ . This reduction converts the entanglement in  $\hat{\rho}$  to entropy, which can be measured directly [1,19], e.g., in the form of linear entropy  $S_L[\tilde{\rho}] = \text{Tr}[\tilde{\rho}(\mathbf{1} - \tilde{\rho})]$ . However, quantifying entanglement in the form of entropy requires care, as also the classical correlation in  $\hat{\rho}$  is converted to entropy. We propose the following entropic entanglement measure

$$E_L[\hat{\rho}] = S_L[\tilde{\rho}] - \min(\text{Tr}[\tilde{\rho}], \text{Tr}[\mathbf{1} - \tilde{\rho}]) S_L[\tilde{\rho}], \quad (8)$$

based on the fact that the entropy gained from the classical correlations is less than the number of electrons or holes times the entropy in  $\hat{\rho}$  [11]. Removing this upper bound of the classical contribution simplifies the evaluation of  $E_L$ , but at the same time makes it less sensitive to detect entanglement in mixed states.

The many-body eigenstate decomposition of  $\hat{\rho}^T$  from the ED solver is shown in Table I. The auxiliary bath orbitals are assigned a spin, but zero orbital angular momentum. In all the studied materials, the ground state configurations maximize  $\langle\hat{S}^2\rangle$  due to the strong Coulomb interaction.

We start by looking at the entanglement in the  $\langle\hat{S}_z\rangle$  and  $\langle\hat{L}_z\rangle$  resolved components  $|\Psi_{m_s}^s\rangle\langle\Psi_{m_s}^s|$  of  $\hat{\rho}^T$ . As seen in Table I, both  $E_G$  and  $E_L$  increase in magnitude as  $|m_s|$  becomes smaller. This trend follows the number of possible ways to distribute the electrons according to their spin [11]. The entanglement in the maximally spin-polarized eigenstate  $|\Psi_s^s\rangle$  depends mainly on the complicated interplay between the Coulomb interaction and the crystal field energies. The maximally spin-polarized ground state of NiO is dominated by a Ni  $d^8$  high spin configuration ( $\uparrow_3^2 \downarrow_3^0$  where the subscript and the superscript stand for the number of  $t_{2g}$  and  $e_g$  electrons respectively). The on-site Coulomb interaction must preserve both  $\langle\hat{S}_z\rangle$  and  $\langle\hat{L}_z\rangle$  which implies that it can not couple this state to any other state. The Coulomb interaction is therefore effectively reduced to a Hartree-Fock term, which makes the eigenstate  $|\Psi_s^s\rangle$  separable. The eigenstates at 80 meV have mainly  $\uparrow_3^2 \downarrow_1^2$  character. Here the Coulomb interaction is allowed to transform these states to  $\uparrow_3^2 \downarrow_1^2$  through pair hopping. Nevertheless, when the maximally spin-polarized states are combined into the density matrix  $\hat{\rho}_s^T$  the entanglement in the states cancels out, giving  $E_G[\hat{\rho}_s^T] = 0.00$ .

TABLE I. Entanglement of the thermal ground state at  $T = 273$  K. The values of  $s$  are defined by  $s(s+1) = \langle \hat{S}^2 \rangle$ , and the degenerate eigenstate  $|\Psi_{m_s}\rangle$  corresponds to  $m_s = -s, \dots, s$  for each value of  $\langle \hat{L}_z \rangle$ .  $E$  (eV) is the relative energy of  $|\Psi_{m_s}\rangle$ , and  $E_G$  and  $E_L$  are defined in the text.

TMO	$E_G[\hat{\rho}_s^T]$	$E_G[\hat{\rho}^T]$	$E_L[\hat{\rho}^T]$	E (eV)	$s$	$\langle \hat{L}_z \rangle$	$E_G[ \Psi_{m_s}^s\rangle\langle\Psi_{m_s}^s ]$					$E_L[ \Psi_{m_s}^s\rangle\langle\Psi_{m_s}^s ]$				
							$m_s = 0$	$\pm 1/2$	$\pm 1$	$\pm 3/2$	$\pm 2$	$\pm 5/2$	0	$\pm 1/2$	$\pm 1$	$\pm 3/2$
MnO	0.00	0.15	-1.67	0.00	5/2	0.00	$m_s = 0$	0.65	0.59	0.00	2.40	1.60	0.00			
FeO	0.00	0.11	-1.40	0.00	2	0.00	0.62	0.58	0.00	2.01	1.51	0.01				
							0.62	0.58	0.00	2.01	1.51	0.01				
CoO	0.02	0.09	-0.81	0.00	3/2	0.00	0.63	0.16		1.64	0.55					
							0.62	0.12		1.57	0.43					
NiO	0.00	0.03	-0.35	0.00	1	0.00	0.50	0.00		1.00	0.00					
							0.50	0.00		1.00	0.00					
							0.63	0.25		1.38	0.75					

The ground state of CoO has mainly a Co  $\uparrow_3^2\downarrow_2^0$  configuration that couples to  $\uparrow_3^2\downarrow_1^1$  through the pair hopping induced by the Coulomb interaction. The pair hopping gives rise to a strong entanglement in  $|\Psi_s^s\rangle$ , and in contrast to NiO, the entanglement is still present in  $\hat{\rho}_s^T$ , giving  $E_G[\hat{\rho}_s^T] = 0.02$ .

The ground state of FeO has primarily a Fe  $\uparrow_3^2\downarrow_0^0$  configuration. The Coulomb interaction is again reduced to a Hartree-Fock term, except when the bath introduces an extra electron in the TM-3d orbitals. As a result the strength of the pair hopping becomes very small, and it gives rise only to a very weak entanglement with  $E_G[|\Psi_s^s\rangle\langle\Psi_s^s|] = 0.003$  and  $E_L[|\Psi_s^s\rangle\langle\Psi_s^s|] = 0.012$ .

The MnO ground state is dominated by the Mn  $\uparrow_3^2\downarrow_0^0$  configuration. Even when one extra electron is introduced from the bath, the Coulomb interaction cannot induce any pair hopping, which makes  $\hat{\rho}_s^T$  fully separable.

The Coulomb interaction gives an additional contribution to the entanglement when two electrons are transferred from the bath to the TM-3d orbitals due to the quadratic increase in repulsion energy. However, for TMOs this contribution is of the order of  $10^{-4}$  for the geometric measure, i.e., too small to be seen in Table I.

Let us now consider the entanglement in the thermal PM ground state  $\hat{\rho}^T$ . For NiO, FeO, and MnO the  $E_G[\hat{\rho}_s^T]$  term in Eq. (7) is zero, and only the  $\langle \hat{S}^2 \rangle$ -dependent part contributes to the entanglement. A single Slater determinant method can therefore *in principle* obtain the maximally spin-polarized states  $|\Psi_{i,s}^s\rangle$ , and then reconstruct the ground states through Eq. (5). However, such an approach would not be adequate for CoO, as  $E_G[\hat{\rho}_s^T]$  is nonzero in this case.

The  $\langle \hat{S}^2 \rangle$ -contribution causes  $E_G[\hat{\rho}^T]$  to increase monotonically from NiO to MnO. A similar trend can in fact also be seen in the relative entropy between the locally projected [11] thermally mixed density operators in LDA and LDA + DMFT [20]. However, due to a strong reduction of the large number of available many-body states in the LDA solution to only a few in the LDA + DMFT solution, the size of the relative entropy reflects mainly the different degree of classical correlation in the two calculations.

A similar trend in the relative entropy is in fact obtained even when the LDA + DMFT ground state is replaced by the separable ground state of a corresponding Hartree-Fock-like LDA +  $U$  simulation.

The proposed  $E_L$  measure was not able to resolve the entanglement in the PM phase, as shown by the negative values of  $E_L[\hat{\rho}^T]$  in Table I. Further refinement of the subtraction of the classical contribution is needed, i.e., by explicitly including the number of orbitals in the procedure [11].

Finally, we note that the PM results can be extrapolated to the type-II antiferromagnetic phase at zero Kelvin, by reducing the thermal ground state to the zero energy eigenstate with the largest magnetic moment. For NiO, FeO, and MnO, these eigenstates are separable, which again makes them describable within theories working with a single Slater determinant, at least in principle. In CoO this state is rather entangled, with a fidelity entanglement of 0.12, which once more puts an upper bound on the accuracy of the single Slater determinant methods for this material. Nevertheless, even though the extrapolated antiferromagnetic ground states of NiO, FeO, and MnO are separable their excited states are in general entangled. Their excitation spectra can therefore not be captured with the single Slater determinant band picture.

We are grateful to the Swedish Research Council, Energimyndigheten (STEM), the KAW foundation and ERC (247062—ASD), for financial support. Calculations have been performed at the Swedish national computer centers UPPMAX and NSC. We would like to thank S. Garnerone and M. I. Katsnelson for useful discussions.

- 
- [1] L. Amico, R. Fazio, A. Osterloh, and V. Vedral, *Rev. Mod. Phys.* **80**, 517 (2008).  
[2] N. F. Mott and R. Peierls, *Proc. Phys. Soc. London* **49**, 72 (1937); B. Brandow, *Adv. Phys.* **26**, 651 (1977); J. Zaanen, G. A. Sawatzky, and J. W. Allen, *Phys. Rev. Lett.* **55**, 418 (1985); M. Imada, A. Fujimori, and Y. Tokura, *Rev. Mod. Phys.* **70**, 1039 (1998).

- [3] V. I. Anisimov, J. Zaanen, and O. K. Andersen, *Phys. Rev. B* **44**, 943 (1991); S. Kobayashi, Y. Nohara, S. Yamamoto, and T. Fujiwara, *ibid.* **78**, 155112 (2008); H. Jiang, R. I. Gomez-Abal, P. Rinke, and M. Scheffler, *ibid.* **82**, 045108 (2010); C. Rödl, F. Fuchs, J. Furthmüller, and F. Bechstedt, *ibid.* **79**, 235114 (2009); A. Fujimori, F. Minami, and S. Sugano, *ibid.* **29**, 5225 (1984); R. Eder, *ibid.* **78**, 115111 (2008); A. Kutepov, K. Haule, S. Y. Savrasov, and G. Kotliar, *ibid.* **82**, 045105 (2010).
- [4] X. Ren, I. Leonov, G. Keller, M. Kollar, I. Nekrasov, and D. Vollhardt, *Phys. Rev. B* **74**, 195114 (2006); J. Kuneš, V. I. Anisimov, A. V. Lukoyanov, and D. Vollhardt, *ibid.* **75**, 165115 (2007); J. Kuneš, A. V. Lukoyanov, V. I. Anisimov, R. T. Scalettar, and W. E. Pickett, *Nature Mater.* **7**, 198 (2008); D. Korotin, A. Kozhevnikov, S. Skornyakov, I. Leonov, N. Binggeli, V. Anisimov, and G. Trimarchi, *Eur. Phys. J. B* **65**, 91 (2008); M. Karolak, G. Ulm, T. Wehling, V. Mazurenko, A. Poteryaev, and A. Lichtenstein, *J. Electron Spectrosc. Relat. Phenom.* **181**, 11 (2010); Q. Yin, A. Gordienko, X. Wan, and S. Y. Savrasov, *Phys. Rev. Lett.* **100**, 066406 (2008).
- [5] A. Georges, G. Kotliar, W. Krauth, and M. J. Rozenberg, *Rev. Mod. Phys.* **68**, 13 (1996); K. Held, *Adv. Phys.* **56**, 829 (2007).
- [6] M. Caffarel and W. Krauth, *Phys. Rev. Lett.* **72**, 1545 (1994).
- [7] S. Y. Savrasov and G. Kotliar, *Phys. Rev. B* **69**, 245101 (2004).
- [8] P. Thunström, I. Di Marco, A. Grechnev, S. Lebègue, M. I. Katsnelson, A. Svane, and O. Eriksson, *Phys. Rev. B* **79**, 165104 (2009).
- [9] A. Grechnev, I. Di Marco, M. I. Katsnelson, A. I. Lichtenstein, J. Wills, and O. Eriksson, *Phys. Rev. B* **76**, 035107 (2007); I. Di Marco, J. Minár, S. Chadov, M. I. Katsnelson, H. Ebert, and A. I. Lichtenstein, *ibid.* **79**, 115111 (2009); O. Grånäs, I. Di Marco, P. Thunström, L. Nordström, O. Eriksson, T. Björkman, and J. Wills, *Comput. Mater. Sci.* **55**, 295 (2012).
- [10] J. M. Wills, M. Alouani, P. Andersson, A. Delin, O. Eriksson, and O. Grechnev, *Full-Potential Electronic Structure Method*, edited by H. Dreysse, Electronic Structure and Physical Properties of Solids: Springer Series in Solid-State Sciences (Springer-Verlag, Berlin, 2010).
- [11] See Supplemental Material at <http://link.aps.org/supplemental/10.1103/PhysRevLett.109.186401> for a full account of the computational details, the implementation of the ED solver, the description of the entanglement search algorithm, and other additional information.
- [12] J. van Elp, R. H. Potze, H. Eskes, R. Berger, and G. A. Sawatzky, *Phys. Rev. B* **44**, 1530 (1991); K. C. Prince, M. Matteucci, K. Kuepper, S. G. Chiuzaibian, S. Bartkowski, and M. Neumann, *ibid.* **71**, 085102 (2005); R. Zimmermann, P. Steiner, R. Claessen, F. Reinert, S. Hüfner, P. Blaha, and P. Dufek, *J. Phys. Condens. Matter* **11**, 1657 (1999); G. A. Sawatzky and J. W. Allen, *Phys. Rev. Lett.* **53**, 2339 (1984).
- [13] J. van Elp, J. L. Wieland, H. Eskes, P. Kuiper, G. A. Sawatzky, F. M. F. de Groot, and T. S. Turner, *Phys. Rev. B* **44**, 6090 (1991).
- [14] E. Bauer and A. Pianelli, *Mater. Res. Bull.* **15**, 177 (1980).
- [15] M. Oku and K. Hirokawa, *J. Appl. Phys.* **50**, 6303 (1979).
- [16] Here we refer to the entanglement between the electrons, and not to the concept of mode-entanglement [1].
- [17] V. Vedral, M. B. Plenio, M. A. Rippin, and P. L. Knight, *Phys. Rev. Lett.* **78**, 2275 (1997).
- [18] R. Jozsa, *J. Mod. Opt.* **41**, 2315 (1994).
- [19] P.-O. Löwdin, *Phys. Rev.* **97**, 1474 (1955).
- [20] K. Byczuk, J. Kuneš, W. Hofstetter, and D. Vollhardt, *Phys. Rev. Lett.* **108**, 087004 (2012).